

Supporting Information

Self-isomerization of nearly planar superatoms formed by actinide embedded gold cluster

Zheng Liu^a†, Yang Gao^b†, Famin Yu^a, Zhonghua Liu^a, Jiarui Li^a, Rui-Qin Zhang^{c}, Yan Xue^{d*} and Zhigang Wang^{a,d*}*

^a Institute of Atomic and Molecular Physics, Jilin University, Changchun 130012, China

^b Center Énergie Matériaux et Télécommunications, Institut National de la Recherche Scientifique (INRS), Canada

^c Department of Physics, City University of Hong Kong, Hong Kong SAR, China

^d College of Physics, Jilin University, Changchun 130012, China

† these authors contributed equally to this work.

*To whom correspondence should be addressed. E-mail: aprqz@cityu.edu.hk (R. Z.); xy4610@jlu.edu.cn (Y. X.) and wangzg@jlu.edu.cn (Z. W.)

Part 1: Computational Method.

Part 2: The charge value in E1, E3, E5, and E6 atom obtained from Hirshfeld charge analysis.

Part 3: Density of states (DOSs) and charge density difference (CDD) of E1, E3, E5, and E6.

Part 4: IR and Raman spectra of E1, E3, E5, and E6.

Part 5: The coordinates of key structures.

Part 1. Computational Method

For Th@Au₁₈ containing actinide and transition metal element, the intense electronic correlations can be effectively controlled by generalized gradient approximation, without increasing computational complexity¹⁻³. The exchange correlation functional BP86 is appropriate for describing the electronic and optical properties of metal–molecule coupled systems^{4, 5}. Considering that the calculations of harmonic frequency with BP86 function are in good agreement with the experimental results due to an error cancellation effect⁶, the BP86 functional is adopted in this work. We also performed the calculations with B3LYP and PBE0 functionals for the energy difference of E1 and E3, as shown in Table S1.

Relativistic corrections of heavy elements have been considered in scalar relativistic (SR) calculations^{7, 8}. We use first-principles with 60-electron relativistic effective core pseudopotential (RECP) in calculations. The optimization calculation is not limited by symmetry. The frequencies of stable structures are calculated to ensure that the imaginary frequencies are suppressed. The Gaussian 09 package⁹ is used to compute the structures and absorption spectra while the Multiwfn 3.7 package¹⁰ is used to analyze the density of states (DOSS), charge density difference (CDD) and Hirshfeld charge analysis.

In view of the need to study different electronic states, we have also studied ultraviolet–visible (UV–Vis) absorption spectra^{11, 12} using time-dependent density functional theory (TDDFT). The zeroth-order regular approximations (ZORA) is used to consider SR and spin–orbit coupling (SOC) effect. The spin-polarized generalized gradient approximation (GGA) with the BP86 exchange-correlation functional is used through the Amsterdam Density Functional (ADF) package¹³. A triple- ζ with polarization functions (TZP) uncontracted Slater-type orbital (STO) basis set is used, where

Au is [1s² – 4d¹⁰] frozen core and Th is [1s² – 4f¹⁰] frozen core.

Table S1. The energy difference of E1 and E3 with BP86, B3LYP, and PBE0 functionals.

	BP86	B3LYP	PBE0
Δ E (eV)	0.05	0.03	0.05
Δ E = E(E3)-E(E1)			

Part 2: The charge value in E1, E3, E5, and E6 atom obtained from Hirshfeld charge analysis.

Table S2. The charge value in E1, E3, E5, and E6 atom obtained from Hirshfeld charge analysis (charge is in e).

Hirshfeld	E1	E3	E5	E6
Au ₆	Th	0.4030	0.3838	0.4035
	Au	0.0293	0.0413	0.0291
	Au	0.0293	0.0414	0.0292
	Au	0.0293	0.0414	0.0291
	Au	0.0293	0.0413	0.0291
	Au	0.0293	0.0413	0.0292
	Au	-0.0290	-0.0335	-0.0289
Au ₁₂	Au	-0.0290	-0.0339	-0.0291
	Au	-0.0290	-0.0339	-0.0291
	Au	-0.0290	-0.0335	-0.0290
	Au	-0.0290	-0.0339	-0.0291
	Au	-0.0290	-0.0335	-0.0290
	Au	-0.0290	-0.0335	-0.0290
	Au	-0.0675	-0.0716	-0.0674
	Au	-0.0674	-0.0716	-0.0673
	Au	-0.0674	-0.0716	-0.0674
	Au	-0.0675	-0.0716	-0.0673
	Au	-0.0674	-0.0716	-0.0673
	Au	-0.0674	-0.0716	-0.0643

Part 3: Density of states (DOSSs) and charge density difference (CDD) of E1, E3, E5, and E6.

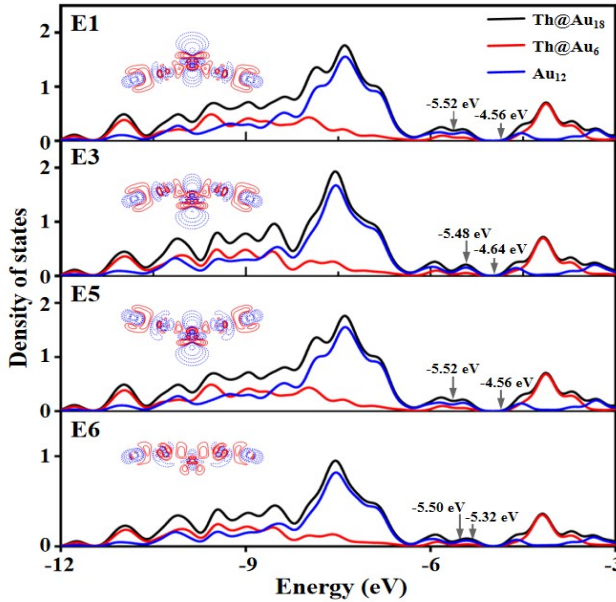


Figure S1. DOSs and CDD of E1, E3, E5, and E6. The black, red and blue lines represent total and partial DOSs ($\text{Th}@\text{Au}_6$ and Au_{12}). Arrows indicate the locations of HOMO and LUMO. The solid red lines represent electron accumulation and dashed blue ones represent electron dissipation.

DOSs is beneficial to display the electronic structure properties of each stable extreme point (E1, E3, E5, and E6), as shown in FIG. S1. The results show that the total and partial DOSs ($\text{Th}@\text{Au}_6$ and Au_{12}) of these structures contributed by these two fragments are hardly changed, and the maximum variation range of the highest occupied molecular orbital-the lowest unoccupied molecular orbital (HOMO-LUMO) gap is about 0.12 eV. These results indicate that nearly planar superatom can not only maintain their electronic structure properties, but also maintain their chemical stability. In addition, CDD analysis shows that electron aggregation exists between Th atom and

gold ring, and the maximum value of electron aggregation appears on Th-Au line. Due to the limitation of outer gold ring, the electron density of Th atom and inner shell increases.

Part 4: IR and Raman spectra of E1, E3, E5, and E6.

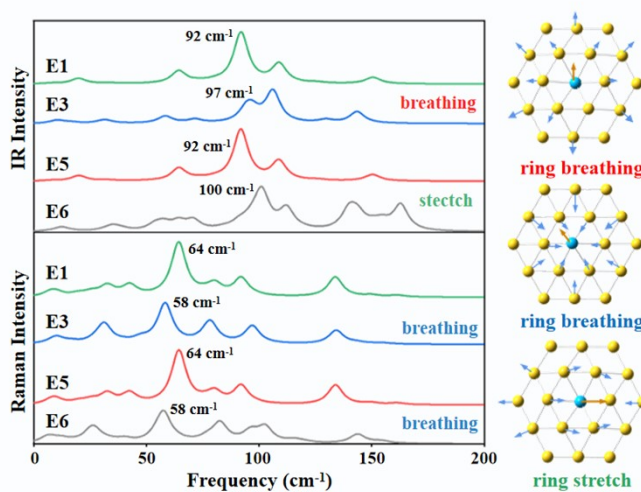


Figure S2. IR and Raman spectra of E1, E3, E5, and E6. The values indicate corresponding peak, and vibration modes of ring breathing and ring stretch are shown on the right.

To provide more information for future experimental verification, we also calculated the vibration spectra of each stable extremum configuration. Th and Au rings have two typical vibration modes (ring breathing and ring stretch). The spectra analysis shows that the ring breathing modes of E1, E3, E5, and E6 belong to Raman and IR activity respectively in the wavenumber range of $58\text{-}64\text{ cm}^{-1}$ and $92\text{-}100\text{ cm}^{-1}$. However, E6 changes into the ring stretch vibration mode in $92\text{-}100\text{ cm}^{-1}$, as shown in FIG. S2. We also find that the activity of Raman spectra decreases first and then increases (nearly

double), and the overall absorption peak shifts first to blue and then to red, with a maximum frequency shift being about 6 cm^{-1} . IR activity also shows the same trend, but the overall absorption peak shift shows an opposite trend (5 cm^{-1}). This small trend change may be caused by the small energy difference between the levels in the isomers. Therefore, we hope that these vibration modes and specific values can provide theoretical basis for the experimental characterization of atomically self-isomerization process.

Part 5: The coordinates of key structures.

Table S3. The coordinate of E1.

	X (Å)	Y (Å)	Z (Å)
1.Th	-0.00000000	-0.00000000	1.46250118
2.Au	0.00000000	2.74234206	0.35011421
3.Au	2.37493789	1.37117103	0.35011421
4.Au	2.37493789	-1.37117103	0.35011421
5.Au	0.00000000	-2.74234206	0.35011421
6.Au	-2.37493789	-1.37117103	0.35011421
7.Au	-2.37493789	1.37117103	0.35011421
8.Au	-4.77121300	0.00000000	-0.24822145
9.Au	4.77121300	0.00000000	-0.24822145
10.Au	-2.38560650	-4.13199167	-0.24822145
11.Au	2.38560650	-4.13199167	-0.24822145
12.Au	-2.38560650	4.13199167	-0.24822145
13.Au	2.38560650	4.13199167	-0.24822145
14.Au	0.00000000	-5.51575924	-0.37528975
15.Au	4.77678762	-2.75787962	-0.37528975
16.Au	4.77678762	2.75787962	-0.37528975
17.Au	-0.00000000	5.51575924	-0.37528975
18.Au	-4.77678762	2.75787962	-0.37528975
19.Au	-4.77678762	-2.75787962	-0.37528975

Table S4. The coordinate of E3.

	X (Å)	Y (Å)	Z (Å)
1.Th	0.00000000	0.00000000	0.25338113
2.Au	-2.40422158	-1.38807798	-0.65737694
3.Au	-2.40422158	1.38807798	-0.65737694
4.Au	0.00000000	2.77615595	-0.65737694
5.Au	2.40422158	1.38807798	-0.65737694
6.Au	2.40422158	-1.38807798	-0.65737694
7.Au	-0.00000000	-2.77615595	-0.65737694
8.Au	2.35389932	-4.07707322	0.22054013
9.Au	-2.35389932	4.07707322	0.22054013
10.Au	4.70779864	-0.00000000	0.22054013
11.Au	2.35389932	4.07707322	0.22054013
12.Au	-2.35389932	-4.07707322	0.22054013
13.Au	-4.70779864	-0.00000000	0.22054013
14.Au	4.74467838	2.73934134	0.39415014
15.Au	0.00000000	5.47868268	0.39415014
16.Au	-4.74467838	2.73934134	0.39415014
17.Au	-4.74467838	-2.73934134	0.39415014
18.Au	0.00000000	-5.47868268	0.39415014
19.Au	4.74467838	-2.73934134	0.39415014

References

1. L. Andrews, B. Liang, J. Li and B. E. Bursten, *J. Am. Chem. Soc.*, 2003, **125**, 3126-3139.
2. H.-S. Hu, F. Wei, X. Wang, L. Andrews and J. Li, *J. Am. Chem. Soc.*, 2014, **136**, 1427-1437.
3. J. Li, H.-S. Hu, J. Lyon and L. Andrews, *Angew. Chem. (International ed. in English)*, 2007, **46**, 9045-9049.
4. J. P. Perdew, *Phys. Rev. B*, 1986, **33**, 8822-8824.
5. A. D. Becke, *Phys. Rev. A*, 1988, **38**, 3098-3100.
6. J. Neugebauer and B. A. Hess, *J. Chem. Phys.*, 2003, **118**, 7215-7225.
7. B. G. Wybourne and L. Smentek, *J. Alloys Compd.*, 2002, **341**, 71-75.
8. J. P. Desclaux and Y.-K. Kim, *J. Phys. B-At. Mol. Phys.*, 1975, **8**, 1177-1182.
9. M. J. Frisch, G. W. Trucks and a. et, *Journal*, 2009.
10. T. Lu and F. Chen, *J. Comput. Chem.*, 2012, **33**, 580-592.
11. A. Laurent and D. Jacquemin, *Int. J. of Quantum Chem.*, 2013, **113**.
12. C. Adamo and D. Jacquemin, *Chem. Soc. Rev.*, 2013, **42**, 845-856.
13. Y. Gao, B. Wang, Y. Lei, B. K. Teo and Z. Wang, *Nano Res.*, 2016, **9**, 622-632.